BRAC University Journal, Vol. IV, No. 1, 2007, pp. 89-96

ON GAMMA-RAY EMISSION FROM PULSAR MAGNETOSPHERE

U. A. Mofiz[1] and Dipen Bhattacharya[2]
Department of Mathematics and Natural Science
BRAC University, 66 Mohakhali C/A
Dhaka-1212, Bangladesh

ABSTRACT

Pulsars, a class of rotating neutron stars, are one of the most interesting objects of nature. Although most pulsars have been detected in the radio range, a handful of them are active in gamma rays. In recent years, significant progress has been made in the understanding of the gamma-ray emission processes from pulsars. In this work, we review the different models that are being put forth to explain the pulsar emission, the relation between pulsars and the unidentified gamma-ray sources observed by the Energetic Gamma Ray Experiment Telescope (EGRET) instrument. We present our recent study of plasma modes in the pulsar magnetosphere and discuss briefly the future of gamma-ray astronomy.

Key words: Gamma ray, pulsar, polar cap, outer gap, EGRET, GLAST

I. INTRODUCTION

When a neutron star is formed from the collapsed remnants of a massive star after a supernova, its rotational speed increases dramatically due to the conservation of its initial angular momentum. The densest stable matter is ascribed to neutron stars and we call a neutron star a pulsar if we observe a beam of radiation in our direction, once for every rotation of the star. The origin of the beam is related to the misalignment of the rotation axis with the magnetic field axis of the neutron star. Although, theorists (Oppenheimer & Volkoff 1939) have speculated about the possible existence of a dense star with neutron matter, it is not until 1967, when Jocelyn Bell Burnell and Antony Hewish noticed periodic spikes in their radio data that pulsars were discovered (Bell, J. et al. 1968).

Only seven pulsars have been detected with high significance in gamma rays (Thompson et al. 1999). Of these, three young and bright gamma-ray pulsars Crab, Vela and Geminga were known since the 1970s. Four more gamma-ray pulsars were added by the detectors on-board the Compton Gamma-Ray Observatory (CGRO) during its ten-year mission (1991-2000). Including the low-significant five or so detections made by CGRO, the total number of known gamma-ray pulsars stands at only 12 or so (Kanbach 2002). However, it is possible that several of the unidentified gamma-ray sources detected by EGRET/CGRO are pulsars that lack radio emission. We should mention, for comparison, the total known pulsars in radio-band exceeds 1500 (Manchester et al. 2005). But as the pulsars that are detected in gamma rays spend most of their spin-down energy in gamma-rays, an understanding of their emission mechanism is crucial for a comprehensive understanding of all pulsars.

Rotation powered pulsars permit a straight-forward determination of the emission parameters that can be deduced from their signature pulsed emission. The Crab and Vela pulsars are long known to be strong sources of pulsed gamma-rays. The EGRET instrument has provided unambiguous and strong evidence for pulsations from five other rotation-powered pulsars. In Figure 1, we show the light curves of the seven gamma-ray pulsars in four electro-magnetic bands: Radio, Optical, X-ray and High Energy Gamma-Ray (>100 MeV). Each panel shows one complete rotation of the star. Most of these pulsars show a double-peaked structure at energies above 100 MeV. The pulsars are arranged according to their rotational age $\tau \sim P/(dP/dt)$ from the youngest Crab ($\tau \sim 10^3$ yrs) to the oldest PSR B1055-52 ($\tau \sim 5 \times 10^5$ yrs). It is now believed that these gamma-rays originate in a large hollow cone above the pulsar surface where high energy particle acceleration and interactions are taking place.

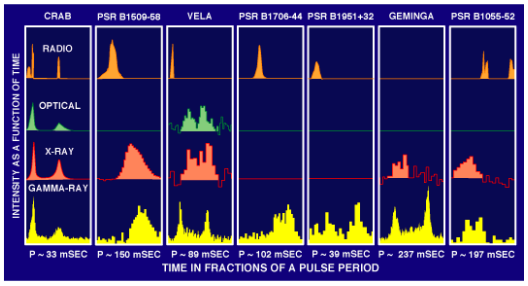

Figure1**:** Light curves of seven gamma-ray pulsars in different energy bands (incorporated from http://heasarc.gsfc.nasa.gov/docs/objects/pulsars, courtesy of D. J. Thompson, GSFC/NASA).

Gamma-ray pulsars tend to have high magnetic fields (~10^{12}-10^{13} G), relatively young ages (~10^4 yrs) and high open field line voltages (~10^{16} V). The rotational energy-loss rate of pulsars is given by

$$dE/dt = \dot{E} = I\Omega\dot{\Omega} = -(2\pi)^2 I\dot{P}/P^3 \qquad (1)$$

where the neutron star is rotating with a frequency of $\Omega = 2P/(dP/dt)$ and a moment of inertia I. For high energy pulsars, some typical values are P ~ 0.1 s, dP/dt ~ 10^{-13} s s^{-1}, I ~ 10^{45} g cm^2 providing for an dE/dt of -4 x 10^{36} ergs s^{-1} which is sufficient to explain the observed gamma-ray luminosities of pulsars (Hirotani 2006). The gamma-ray pulsars usually have the highest value of the parameter $(dE/dt)d^{-2}$ where d is the distance to the pulsar.

Rotating and conducting neutron stars can be understood within a model of a unipolar inductor generating very large **v x B** electric fields capable of pulling charges from the neutron star surface against the force of gravity. Hence, the magnetosphere of the neutron star is filled with charge separated plasma that tends to oppose the induced **v x B** electric field. The resulting field is capable of shorting out the $E_{\|}$ (parallel to the magnetic field) everywhere except a few locations. Two places where strong $E_{\|}$ may accelerate particles and generate radiation are i) near the magnetic poles (polar caps) or ii) in the outer magnetosphere (outer gaps). In this paper, we will summarise pulsar gamma-ray generation models, including the polar cap and the outer gap models and some observational verificationss of those models.

II. POLAR CAP MODEL

A. Primary Electrons and Acceleration at the Polar Cap

The location of the gamma ray emission in the polar cap model lies in the "open field line" region of the pulsar magnetosphere. The open field lines are those which do not return to the neutron star surface within the co-rotation radius of pulsar. The co-rotation radius is the radius at which objects co-rotating with the pulsar approach the speed of light. The locus of these points is conventionally referred to as the *light cylinder*. Figure 2 shows the open field line region and light cylinder for a dipole field geometry. The polar cap is defined as the place from where the open field lines originate at the surface of the neutron star.

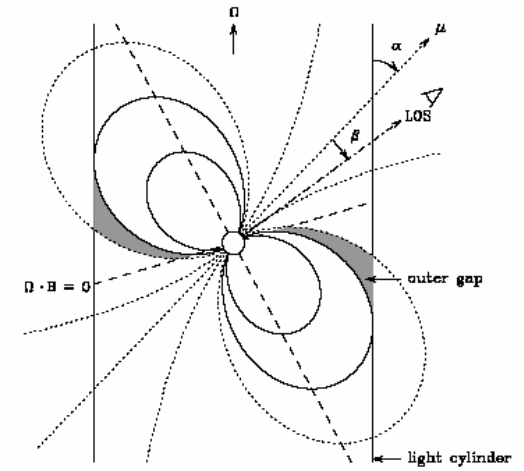

Figure 2**:** Pulsar magnetosphere for a dipole field geometry. The polar cap acceleration zones lie near the surface of the neutron star at the magnetic polar caps and the outer gap acceleration zones extend from the null-charge surface which is defined by $\mathbf{\Omega \cdot B = 0}$ and the light cylinder along the last closed field lines.

Goldreich and Julian (1969) showed that a totally evacuated co-rotating magnetosphere cannot exist around a rapidly rotating neutron star. Strong electric fields will be generated with sufficiently large components perpendicular to the neutron star surface to rip material from the surface to generate a plasma which fills the magnetosphere. The resulting charge density of this plasma is simply that required to cancel out the induced electron field due to the rotating magnetic field:

$$\rho_{GJ} = -\frac{1}{2}\nabla\cdot\frac{(\vec{\Omega}\times\vec{r})\times\vec{B}}{2\pi c} \cong -\frac{\vec{\Omega}\cdot\vec{B}}{2\pi c} \qquad (2)$$

Ruderman and Sutherland (1975) proposed a model of pulsar emission based on the formation of vacuum gaps near the polar cap. In their model, the work function for ions on the stellar surface is assumed to be sufficiently large to prevent them from being stripped from the surface and shorting out the potential that is formed. Other models also calculated space charge limited flow and found potentials as large as the Rutherman-Sutherland potential (Arons 1983, Muslimov and Tsygan 1992).

Mofiz and Ahmedov (2000) consider electrostatic plasma modes along the open field lines of pulsar. Goldreich-Julian charge density in general relativity with zero inclination of the pulsar is analysed in this paper where the dragging of inertial frame and the effect of general relativity are fully considered. Since pulsars having smaller obliquity have larger accelerating drops and thus are favored for gamma-ray pulsar models (Daugherty and Harding 1994, 1996; Dermer and Sterner 1994), this analysis is confined with the zero inclination of the pulsar. Both linear and nonlinear modes are considered and it is found that

1. Goldreich –Julian charge density is maximum in the polar cap region and remains almost the same in a certain extended region of the pole. The charge density decays with the distance away from the surface of the star.
2. Plasma oscillation along the field lines resembles the gravitational redshift near Schwarzschild radius.
3. Plasma modes grow near the gravitational radius in the black hole environment.

Study of plasma modes along the field lines is boosted by the pioneering works of Goldreich and Julian (1969), Sturrock (1971), Mestel (1971), Ruderman and Sutherland (1975), and Arons and Scharlemann (1979). The subsequent achievements and some new ideas are reviewed by Arons (1991), Michel (1991), Mestel (1992), and Muslimov and Harding (1997). Although a self-consistent pulsar magnetosphere theory is yet to be developed, the analysis of plasma modes in the pulsar magnetosphere based on the above mentioned papers provides firm grounds for the construction of such model.

Mofiz 2004 studies Alfvén wave propagation in the polar cap region of isothermal magnetosphere of a compact gravitating object like pulsar or black hole. It is found that Alfvén speed increases steeply near the horizon, reaches a maximum, then decreases very sharply close to the event horizon. This unique feature of Alfvén speed near the polar region creates the phenomenon of wave trapping by the plasma within a distance of several Schwarzschild radius, which depends sensitively on the temperature of the plasma.

For further study of plasma dynamics in the pulsar magnetosphere or in the black hole environment, we plan to extend our earlier investigations on soliton (see Mofiz 1989a, 1989b, 1990, 1997; Mofiz, de Angelis and Forlani 1985; Mofiz, Tsintsadze, and Tsintsadze 1995) propagation along the open field lines of strongly gravitating objects.

B. Curvature Radiation and Pair-Production in Strong Magnetic Fields

The primary source of high energy radiation in the polar cap model is curvature radiation. The very high energy electrons and positrons injected at the polar cap along the open field lines produce curvature radiation. The spectrum of this radiation is given by

$$\frac{dI}{d\omega} = \sqrt{3}\frac{e^2}{c}\gamma\frac{\omega}{\omega_c}\int_{\omega/\omega_c}^{\infty} K_{5/3}(x)dx = \sqrt{3}\frac{e^2}{c}\gamma F_{syn}(\omega/\omega_c) \quad (3)$$

where $K_{5/3}$ is a modified Bessel function of the third kind, $\omega_c = 3c\gamma^3/2\rho_c$ is the critical frequency, $\gamma = E/m_ec^2$ is the electron energy, ρ_c is the curvature radius at the emission point, and $F_{syn}(x)$ is defined as

$$F_{syn}(x) \equiv x\int_x^{\infty} K_{5/3}(x')dx' \qquad (4)$$

(Jackson 1975). For electrons with $\gamma \approx 10^7$, the critical or cut-off energy will be $\varepsilon_c \equiv \hbar\omega_c \cong 10$ GeV so that a break in the emergent spectra will occur around this energy.

The curvature radiation is emitted parallel to the electron trajectory and therefore will be initially beamed along the local magnetic field. As the

radiation propagates through the magnetosphere, it will develop a component of its momentum which is perpendicular to the local field. If the field intensity is strong enough, the photon will interact with the field and convert to an electron-positron pair. This is known as Sturrock process since he was the first to apply it to the problem of radio emission from pulsars (Sturrock 1971).

The rate of pair production, $\varsigma(\gamma B \rightarrow e^+e^-)$ is given by

$$\varsigma = 0.23\frac{c}{\alpha}\frac{B}{B_{crit}}\frac{(B^2-E^2)}{(B^2-\eta_x BE)}\left(\left(\eta_x-\frac{E}{B}\right)^2+\eta_y^2\left(1-\frac{E^2}{B^2}\right)\right)^{1/2} \times\exp\left\{-\frac{8}{3}\left(\frac{m_e c^2}{E_\gamma}\right)\frac{B_{crit}}{B}\left(\left(\eta_x-\frac{E}{B}\right)^2+\eta_y^2\left(1-\frac{E^2}{B^2}\right)\right)^{-1/2}\right\} \quad (5)$$

where c is the speed of light, α is the fine structure constant, λ_e is the de Broglie wavelength of the electron, m_e is the electron rest mass, E and B are the local electric and magnetic fields, E_γ is the photon energy, $\eta = (\eta_x, \eta_y, \eta_z)$ are the direction cosines of the photon in the frame where $E \parallel \hat{v}$ and $B \parallel \hat{z}$, and $B_{crit} = 2\pi m_e^2 c^3/eh$.

C. Synchrotron Radiation and Electromagnetic Cascades:

The resulting pairs produced by the Sturrock process will typically have substantial component of their momentum perpendicular to the local magnetic field. Consequently, they will be strong emitters of synchrotron radiation. The spectrum of synchrotron photons for a very energetic electron with energy E_e in the frame in which the electron momentum is purely transverse to the magnetic field is given by

$$I(E_{e,}\omega, B) = \sqrt{3}\alpha\frac{m_e c^2}{\lambda_e}\left(\frac{\Gamma}{E_e}\right)\left(1-\frac{\hbar}{E_e}\right)F_{syn}(\zeta) \quad (6)$$

where

$$\Gamma = \left(\frac{E_e}{m_e c^2}\right)\left(\frac{B}{B_{crit}}\right),$$

$$\zeta = \frac{y}{2+3\Gamma(1-y)},$$

$$y = \frac{\omega}{\omega_{crit}},$$

$$\hbar\omega_{crit} = E_e\frac{3\Gamma}{2+3\Gamma}.$$

These synchrotron photons will also be subject to the same pair production process that the curvature photons were. A pair photon cascade will develop and the resulting radiation will comprise the high energy flux seen on Earth.

It is either the inverse-Compton (IC) or the curvature-radiation (CR) photons that control the production of pairs that ultimately screen the radiation field. Harding and Muslimov (1998) found that in pulsars, where IC-controlled acceleration zones are stable, particles' energies are limited to Lorentz factors of 10^5 to 10^6. In this case, IC is both the dominant primary radiation mechanism and initiator of the pair cascade (Sturner and Dermer 1994). In pulsars, where IC photons cannot screen the accelerating field, the primary particles continue to accelerate up to Lorentz factors of ~ 10^7. CR is then the dominant primary radiation mechanism and initiates the pair cascade. The emergent cascade spectrum is dominated by synchrotron radiation from the pairs; the pairs can also resonant-scatter the soft thermal photons from the neutron star surface, losing most of the remaining parallel energy they could not lose via synchrotron emission (Zhang and Harding 2000).

III. OUTER GAP MODEL

A vacuum gap (outer gap) may develop in outer magnetosphere between the last open field line and the null charge surface ($\vec{\Omega}\cdot\vec{B}=0$) in charge separated magnetospheres. The outer gap models for gamma-ray pulsars are based on particle acceleration in this outer gap. We already mentioned that a neutron star could be considered as an oblique rotator with a strong magnetic field B and angular spin Ω that gives rise to a charge density of $\vec{\Omega}\cdot\vec{B}/2\pi c$ in the corotating magnetosphere.

This geometry also gives rise to a quadrupolar electric field for which $\vec{E}\cdot\vec{B}\neq 0$. The regions where charge density vanishes are given by

$\vec{\Omega} \cdot \vec{B} = 0$ within the light cylinder; at the radius of the light cylinder (radius = c/Ω) the tangential field line velocity approaches the speed of light. The open magnetic field lines intersect the null-charge surface $\vec{\Omega} \cdot \vec{B} = 0$ within the light cylinder; the charge density changes sign at this surface. The outer gaps arise because charges escaping through the light cylinder along open field lines above the null charge surface cannot be replenished from the neutron star surface (Cheng, Ho and Ruderman 1986). A removal of charged particles of one sign from the region outside the $\vec{\Omega} \cdot \vec{B} = 0$ cone would give rise to an electric field which moves charged particles of opposite sign away from the other side of the cone, pushing them back towards the stellar surface. This leaves a region of depleted charge and strong $\vec{E} \cdot \vec{B}$ about the null charge cone.

The large potential drop that generates this strong electric field across the open field lines of the magnetosphere is a function of the star's surface magnetic field B_s, radius R and rotation rate Ω and is given by

$$\Delta V \approx \frac{\Omega^2 B_S R^3}{c^2} \qquad (7)$$

where the expression $B_S R^3$ represents the magnetic dipole moment of the star.

The outer gap model predicts the spectral flattening of gamma rays below a certain minimum energy (E_{min}) and a spectral cutoff above a certain maximum energy (E_{max}). The former implies gamma rays are not produced in low energies according to a power law model and the latter implies there is a maximum energy. The maximum energy of gamma rays depends on the field strength in the gap and the period of the pulsar. Strong magnetic field tends to suppress gamma rays through e^+ / e^- pair production. However, magnetic field strength in the outer gap should be small relative to the polar cap field strengths as the outer gap is further from the stellar surface. This might allow the TeV gamma rays to escape the star (Hirotani and Shibata 2001).

In Vela-type pulsars primary gamma rays (from inverse Compton scattering) with energies E ~ 10^{13} eV (or 10 TeV) encounter low-energy photons (with energies less than 0.15 eV) to produce secondary electrons through e^+ / e^- production. These electrons then radiate synchrotron secondary gamma rays over a wide spectrum of energies where the range of synchrotron energies is determined by the available time for a secondary electron to radiate down to a minimum energy of about 10 MeV, below which the spectrum flattens. For Vela-type pulsars the maximum synchrotron energy from secondary e^+ / e^- in the outer gap is about 20 GeV.

However, the cycle is not done until the secondary synchrotron gamma rays give rise to low-energy tertiary e^+ / e^- pairs. The synchrotron radiation from these pairs results in infrared and optical photons within the outer gap so that primary TeV gamma rays can again result from inverse Compton scattering and secondary TeV e^+ / e^- pairs from TeV photon-infrared photon collisions. As this bootstrap process happens relatively far from the stellar surface, TeV gammas may escape magnetic pair production due to the weaker magnetic field.

As a pulsar ages its period increases and its E_{min} increases until it becomes comparable to E_{max} at which point the outer gap ceases to exist and the gamma-ray production is turned off. In older Vela-like pulsars, the outer gap model is able to explain the phase-averaged spectral shapes between the optical and GeV energies. The e^+ / e^- pairs were assumed to come from interaction of primary particle inverse Compton photons with infrared photons, which predicts a higher flux of TeV gamma rays, but so far only upper limits have been obtained (Albert et al. 2007). The TeV upper limits indicate that the gaps are too small to account for the observed luminosity below GeV energies. In young Crab-like pulsars, the e^+ / e^- pairs are produced by curvature photons from the primary particles interacting with non-thermal synchrotron X-rays from the same pairs.

IV. OBSERVATIONS

In Figure 3, we show the multi-wavelength spectra for the pulsed emission of gamma-ray pulsars as compiled by Thompson et al. (1999). The intensities are plotted as a function of frequency/energy in such a way (frequency times flux or νF_ν) that the curves display the total radiated power per logarithmic unit interval of frequency (lnν). It is evident from the figure that the radiation from these pulsars is dominated by X- and gamma-ray emission and there is a cut-off or turn-over of the spectra at GeV energies.

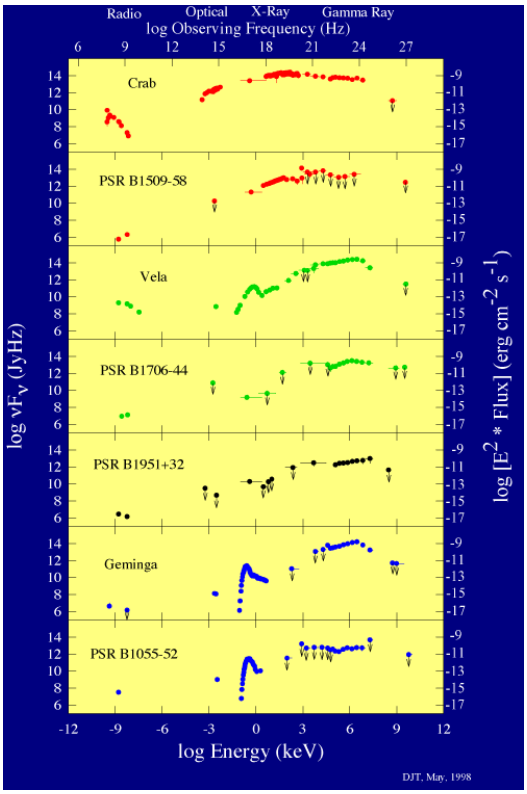

Fig. 3: These energy spectra of seven high-energy pulsars are shown in a format that plots the power seen per decade of energy observed in units of JyHz. All these pulsars have their maximum output in the hard X-ray to gamma-ray energy band, displaying vastly more energy at high energies than in the optical or radio bands. At the highest energies, all these pulsars show a drop-off in their output. The figure is reproduced from http://heasarc.gsfc.nasa.gov/docs/objects/pulsars/pulsars_spec.html (courtesy of D. J. Thompson, GSFC/NASA).

The Crab has a strong unpulsed component at high energies that is believed to be coming from the inner Crab Nebula as synchrotron radiation (below a few GeV) and as inverse Compton radiation up-scattered from optical photons up to TeV energies. The spectrum of PSR B1509-58 has a low energy cut-off ~ 10 MeV which has been explained as an absorption effect for high energy photons in a strong magnetic field (~2 x 10^{13} gauss). For Geminga, the power in optical and radio emissions is lower than the gamma-ray emission by more than six orders of magnitudes.

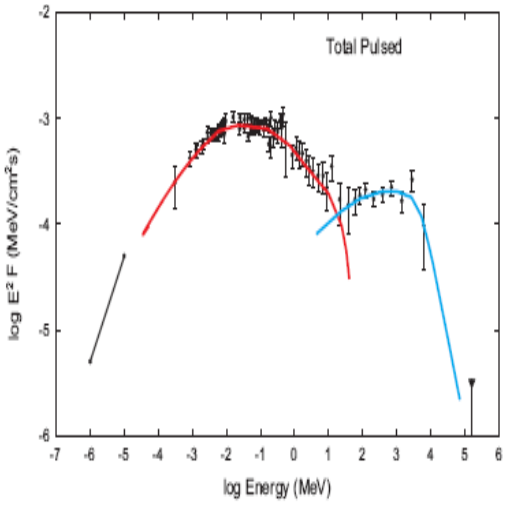

Figure 4**:** Crab pulsar pulsed emission. Incorporated from Kanbach (2002), the graph shows data points for the Crab pulsar pulsed emission (Kuiper et al. 2001). The continuous line shows the theoretical spectra corresponding to emission via the synchrotron process (low energy peak) and the inverse Compton or curvature radiation peak at higher energies.

In Figure 4, we show the pulsed spectra of the Crab pulsar. The pulsed Crab emission has a low energy peak around 100 keV possibly of a synchrotron origin. Very energetic electrons (γ~10^6-10^7) in the outer magnetosphere with a weak magnetic field (~1 G) or electrons with γ~10^2-10^3 in inner strong polar fields (~10^8 G) can provide such an emission. The high energy peak at ~ 1-10 GeV could result from IC scattering of energetic electrons where electrons with Lorentz factors of 10^4 could boost 10 eV photons into GeV energies. Even though the Crab Nebula was detected at very high energies (up to 10 TeV) with instruments like Whipple, HESS and MAGIC, the emission from the Crab pulsar itself was not detected above 100 GeV (Albert et al. 2007). Recent outer gap models of Hirotani (2007) have downgraded the pulsed component from the Crab pulsar due to dominant gamma-gamma absorption process.

V. EGRET UNIDENTIFIED SOURCES

Young radio pulsars are suggested to be one of the potential counterparts of many EGRET unidentified gamma-ray (EUI) sources (Yadgaroglu and Romani 1997, Harding and Zhang 2001). The LogN-LogS curves of radio pulsars, both young and old, can be fitted with power laws

that have indices close to -1.0. This would seem to indicate that the pulsar population is uniformly distributed in the Galactic thin disk. On the other hand, we find the LogN-LogS curve of the EUI sources has a very steep index ~ -2.7 (Bhattacharya et al. 2003) which is not indicative of a uniform disk population (e.g. pulsars). The steep index can be understood in terms of a model where sources are not uniformly distributed.

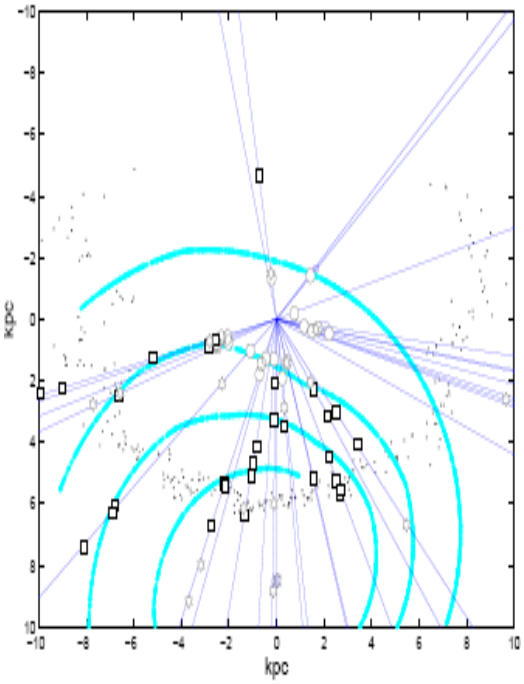

Figure 5. Positional coincidences with pulsars, SNRs and OBAs.

We find that the EUI source distribution closely follows the Galactic spiral arm structure. This seems to satisfy the hypothesis that the EUI sources arise due to energetic interactions with molecular clouds that reside in the spiral arms. Furthermore, the luminosity distribution of the unidentified sources show a two-population Gaussian distribution (Miyagi et al. 2005). We find a combined distribution of OB stellar associations (OBA), SNR and superbubbles interaction with molecular clouds within the spiral arms which are most likely the counterparts of the unidentified sources. Figure 5 is the face-on map of OB stellar associations (small circles), supernova remnants (pointed stars) and pulsars (squares) which have positional coincidences with EUI sources; the direction of the EUI sources are shown by straight lines). Positional coincidences with OBAs, SNRs and superbubbles are relatively close to the Sun, pulsar coincidences within 3 kpc of the Sun are relatively few. Recent radio pulsar survey of 56 EUI sources did not find a strong correlation between millisecond pulsars and EUI sources (Crawford et al. 2006).

VI. CONCLUSION

In this paper we have reviewed different models of gamma-ray emissions from pulsar magnetosphere. The concerned models are polar gap and outer gap. There is another model which is known as slot gap to be treated later. In all models it is found that the emission occurs in plasma due to acceleration of particles developed in the gap. Therefore, here we gave brief review of our earlier works related to plasma modes in the pulsar magnetosphere. Some recent observation of gamma-ray emissions are also provided here.

The next generation of gamma-ray telescopes, especially the Gamma-Ray Large Area Space Telescope (GLAST) experiment due to be launched in late 2007, are expected to be much more sensitive and should discover 30-100 new gamma-ray pulsars based on the catalog of radio pulsars. Detailed spectroscopic studies of the pulsed emission by GLAST and other ground-based experiments with lower thresholds will hopefully resolve the origin of high energy pulsed emission. Furthermore, equipped with relatively higher angular resolutions, these instruments will be able to resolve the identity of the EGRET unidentified gamma-ray sources

[1]Email: uamofiz@yahoo.com
[2]Email: dipenb@bracuniversity.ac.bd; also at IGPP, UC Riverside, CA 92521, USA

REFERENCES

Albert, J., Aliu, E., Andernub, H., Antoranz, P., Armada, A., Baixeras, C., Barrio, J. A., Bartko, H., Bastieri, D., Becker, J. K., Bednarek. W., Berger, K., Bigongiari, C., Biland, A., Bock, R.K., Bordas, P., Bosh-Ramon, R., Bertz, T., Britvitch, I., Camara, M., Carmona, E., Chilingarian, A., Coarsa, J. A., Commichau, S., Conteras, J. L., Cortina, J., Costado, M. T., Curtef, V., Danielyan, V., Dazzi, F., De Angelis, A., Delgado, C., De Los Reyes, R., Lotto, B. De., Domingo-Santamaria, E., Dorner, D., Doro, M., Errando,

M., Fagilini, M., Ferenc, D., Fernandez, E., Firpo, R., Flix, J., Fonseca, M. V., Font, L., Fuchs, M., Galante, N., Garci'a-Lo'pez, R., Garczarczyk, M., Gaug, M., Giller, M., Goebel, F., Hakobyan, D., Hayashida, M., Hengstebeck, T., Herrero, A., Höhne , D., Hose, J., Hsu, C. C., Jacon, P., Jogler, T., Kosyara, R., Kranich, D., Kritzer, R., Laile, A., Lindfors, E., Lombardi, S., Longo, F., López, J., López, M., Lorenz, E., Majumdar, P., Maneva, G., Mannheim, K., Mansutti, O., Marrioti, M., Matínez, M., Mazin, D., Merck, C., Meucci, M., Meyer, M., Miranda, J. M., Mirzoyan, R., Mizobuchi, S., Moraleyo, A., Nieto, D., Nilsson, K., Ninkovic, J., Ona-Wilhelmi, E., Otte, N., Oya, I., Panque, D., Pannielo, M., Paoletti, R., Pardes, J. M., Pasanen, M., Pascoli, D., Pauss, F., Pegna, R., Persic, M., Peruzzo, L., Piccioli, L., Poller, M., Prandini, E., Puchades, N., Raymers, A., Rhode, W., Ribó, M., Rico, J., Rissi, M., Robert, A., Rügamer, S., Saggion, A., Sánchez, A., Sartori, P., Scalzotto, V., Scapin, V., Schimitt, R., Schweizer, T., Shayduk, M., Shinozaki, K., Shore, S. N., Sidro, N., Sillanpää, A., Sobczynska, D., Stamerra, A., Stark, L. S., Takalio, L., Temnikov, P., Tescaro, D., Teshima, M., Tonello, N., Torres, D.F., Turini, N.,

Vankov, H., Vitale, V., Wagner, R. M., Wibig, T., Wittek, W., Zandanel, F., Zanin, R., Zapatero, J. 2007, arXiv:0705.3244v1.

Arons, J. and Scharlemann, E. T. 1979, ApJ, 231, 854.

Arons, J., 1983, ApJ, 266, 215.

Bell, J., Hewish, A.,Pilkington, J. D. H.; Scott, P. F. and Collins, R. A., 1968, Nature, 217, 709.

Bhattacharya, D., Akyüz, A., Miagi, T., Samini, J., and Zych, A. 2003, A&A, 404, 163.

Cheng, H., Ho, C. and Ruderman, M. 1986, ApJ, 300, 500.

Crawford F., Roberts, M. S. E., Hessels, J. W. T., Ranson, S. M., Livingstone, M., Tam, C. R., Kaspi, V. M. 2006, ApJ, 652, 1499.

Daughterty, J. K., and Harding, A. K. 1994, ApJ, 429, 325

_____. 1996, ApJ, 458, 278.

Dermer, C. D., and Sterner, S. J. 1994, ApJ, 420, L75.

Goldreich, P., and Julian, W. H. 1969, ApJ, 157, 869.

Harding, A. and Muslimov A. 1998, ApJ, 508, 328.

Harding, A.K., and Zhang, B. 2001, ApJ, 548, L37.

Hirotani, K. and Shibata, S., 2001, ApJ, 558, 216.

Hirotani, K. 2007, astro-ph/0701676.

Jackson, J.D., 1975, Classical Electrodynamics, Wiley Publishing, New York.

Kanbach, G. 2002, astro-ph/0209021v1.

Kuiper, L.,Hermsen, W., Cusumano, G., Diehl, R Schonfelder, V., Strong, A., Bennet, K. McConnel, 2001astro-phys/0109200.

Manchester, R. N. Hobbs, G. B. Teoh, A., and Hobbs, M 2005, AJ, 129, 1993.

Michel F. C. 1991, ApJ, 383, 808.

Miyagi, T., Bhattacharya, D. and Zych, A. D. 2005, ApSS, 297, 191.

Mestel, L. 1971, Nature, 233, 149.

Mofiz, U. A. and Ahmedov B. J. 2000, ApJ, 542, 484.

Mofiz, U. A. 1989a, Phys. Rev. A, 40, 2203.

Mofiz, U. A. 1989b, Phys. Rev. A, 40, 6752.

_____.1990, Phys. Rev. A, 42, 960.

_____.1997, Phys. Rev. E, 55, 5894.

--------. 2004, Phys. Plasmas, 11, 3898.

Mofiz, U. A., De Angelis U., and Forlani, A. 1985, Phys. Rev. A, 31, 951.

Mofiz, U. A., Tsintsadze, L. N., and Tsintsadze, N. L. 1995, Phys. Scr., 51, 390.

Muslimov, A. and Tsygan, A. I., 1992, MNRS, 255, 61.

Muslimov A. and Harding A,. 1997 ApJ, 485, 735.

Oppenheimer, J. R. and Volkoff, G. M. 1939, Phys. Rev., 55, 374.

Ruderman, M. A. and Sutherland, P. G. 1975, ApJ, 196, 51.

Sturner, S. J. and Dermer, C. D. , 1994, ApJ, 420. L79.

Sturner S. J. and Dermer C. D. 1996, ApJ, 420, L79.

Sturrock, P. A. 1971, ApJ, 164, 529.

Thompson, D. J., Balles, M., Bertsch, D. L., Cordes, J., D'Amico, N., Esposito, J. A., Finley, J., Hartman, R. C., Hermsen, W., Kanbach, G., Kaspi, V. M., Kniffen, D. A., Kuiper, L., Lin, Y. C., Lyne,A., Manchester, R., Matz, S. M., Mayer-Hasselwander, H. A., Michelson, P. F., Nolan, P. L., Pohl, M., Ogelman, H., Ramanamurthy, P. V., Sreekumar, P., Reimer, O., Taylor, J. H., and Ulmer M. 1999, ApJ, 516, 297.

Yadgaroglu, I.A. and Romani, R.W. 1997, ApJ, 476, 347.

Zhang, B. and Harding, A. K. 2000, ApJ, 532, 1150.